Unmanned Systems, Vol. 4, No. 3 (2016) 213–226
© World Scientific Publishing Company
DOI: 10.1142/S2301385016500072

UNMANNED SYSTEMS
http://www.worldscientific.com/worldscinet/us

Active Control of a UAV Helicopter with a Slung Load for Precision Airborne Cargo Delivery

Keeryun Kang*,‡, J. V. R. Prasad†,§, Eric Johnson†,¶

*Agency for Defense Development, 111 Sunam-Dong, Yuseong, Daejeon 305-152, Korea (Reblic of)

†School of Aerospace Engineering, Georgia Institute of Technology, 270 Ferst Drive, Atlanta, GA 30332-1050, USA

Un. Sys. 2016.04:213-226. Downloaded from www.worldscientific.com
by NATIONAL UNIVERSITY OF SINGAPORE on 12/14/16. For personal use only.

An active controller for a UAV helicopter carrying a slung load is described in this paper. The objective of the controller is to allow the UAV to safely transport a slung load and to place it precisely on a moving ground platform such as a moving truck or a ship. In order to fulfill this objective, an active slung load controller is synthesized that forms an outer loop in providing trajectory commands to an existing automatic flight control system (AFCS) of an unmanned helicopter. The synthesized controller consists of three sub-components; first a target position tracker which generates position tracking commands, second a load oscillation controller which generates load oscillation damping commands, and third an adaptive neural network which compensates for uncertainties associated with flight environment and/or modeling errors. A linear proportional-plus-derivative (PD) controller is used for the target position tracking control. A nonlinear controller based on feedback linearization of the slung load dynamics is used for the load oscillation control. A single hidden layer neural network with an adaptive gain update is used for uncertainty compensation. The proposed controller is evaluated in simulations within the Georgia Tech UAV Simulation Tool (GUST) and inflight tests using the GTMax UAV helicopter test-bed. Both simulation and flight test results are presented to demonstrate the effectiveness of the proposed controller in dampening of load oscillations while simultaneously reducing position errors relative to a virtual moving ground platform, in the presence of random ground vehicle motion, wind gusts, and modeling errors.

Keywords: Autonomous cargo delivery; slung-load control; nonlinear oscillation controller; adaptive neural network.

US

1. Introduction

From the beginning of the idea of using a helicopter as a cargo carrier, the unique flying capability of a helicopter with external cargo has proven its versatility in both military and civil operations. However, carrying an externally suspended cargo, usually known as a slung load, poses its own difficulty to helicopter pilots. A slung load increases the mission gross weight of a helicopter and the oscillatory behavior of slung load can alter the flight characteristics resulting in a narrowed flight envelope. In addition, any unstable slung load oscillations, if not well damped, may pose a danger to flight safety. It is well known that because of the tight coupling between the slung load and vehicle motions, pilot inputs need to be carefully tailored in order to prevent potential pilot induced oscillations.

Early studies of slung load systems using dynamic modeling, wind tunnel tests, and flight tests were primarily focused on flight safety. The aim of those studies was often to determine safe operational limits on the flight envelope of a helicopter, and to determine the design specification on the main parts of the slung load system, such as cable, cable sling, etc. [1]. Cicolani's work on mathematical modeling of a slung load system provided a basis for much of the slung load system simulations [2, 3]. Besides mathematical modeling, some of the past studies have also addressed various control issues associated with slung load systems. Active damping of

Received 11 September 2014; Revised 30 May 2016; Accepted 30 May 2016; Published 19 October 2016. This paper was recommended for publication in its revised form by editorial board member, Feng Lin.
Email Addresses: ‡*keeryun@gmail.com*, §*jvr.prasad@ae.gatech.edu*, ¶*eric.johnson@ae.gatech.edu*

Un. Sys. 2016.04:213-226. Downloaded from www.worldscientific.com
by NATIONAL UNIVERSITY OF SINGAPORE on 12/14/16. For personal use only.

slung load motion using aerodynamic actuators attached on the load is an example [4]. However, from a practical point of view, controlling the slung load by the vehicle motion without any actuators on the load is advantageous. Therefore, recent studies on slung load control have focused on control of a helicopter itself, for example, the successful case of a small scale UAV helicopter utilizing input shaping and delayed feedback control for load damping [5, 6]. While most of the previous studies were more interested in stabilizing the load motion rather than precisely controlling the position of the load, a recent study used a small scale UAV helicopter to show that it was possible to control the load position along a preplanned trajectory [7].

The objective of the current study is to develop an active controller for a UAV helicopter which can stabilize the oscillation of an external payload for its delivery onto a moving ground platform. This requires that not only the load motion is well damped but also the load motion is controlled within a small range of error over a moving ground target. For this purpose, this paper proposes an active slung load controller that forms an outer loop in providing trajectory commands to an existing automatic flight control system (AFCS) of an unmanned helicopter. The main contributions of the paper are synthesis of the slung load controller and simulation and flight test evaluations of the developed controller using the Georgia Tech Unmanned Aerial Vehicle Testbed.

The slung load controller consists of a target position tracker and an adaptive neural net based nonlinear slung load damper. The target position tracker is made up of a linear proportional-plus-derivative (PD) controller which generates an acceleration command to track a moving target. The nonlinear slung load oscillation damper is based on feedback linearization of the nonlinear dynamics of the slung load system. As these two controllers can act against each other, the gain selection for these two controllers needs to be made such that any undesirable coupling between them is eliminated [8].

Although a careful selection of the gains of the target position tracker and the load oscillation damper is needed to guarantee stability of the closed loop system, the overall performance of the controller may degrade in the presence of uncertainties associated with environmental conditions and/or errors in the slung load parameter estimates needed for control. For example, errors between the estimated and the real values of the slung load mass, aerodynamic characteristics, etc., and wind gusts may cause performance deterioration in target position tracking. For this reason, an adaptive neural net is included to compensate for these types of uncertainties.

The arrangement of the paper is as follows. First, a detailed development of the proposed slung load controller is presented. Next, results from detailed simulation evaluations are presented, which are followed by preliminary flight test evaluation results. These are followed by concluding remarks and recommendations for future work.

2. Controller Synthesis

2.1. *The basic approach*

Figure 1 illustrates the intended conceptual operation of the proposed active controller. As shown in the figure, basic operation of the controller is to regulate the load position error with respect to the reference trajectory of the moving ground target by controlling the helicopter trajectory, while suppressing any load oscillations.

The active slung load controller receives the target position to be tracked either as command inputs from a load operator in a manned system or from an onboard system tracking the ground vehicle in an autonomous system. The load position commands are converted by the active slung load controller into appropriate vehicle trajectory commands in the form of either position commands or velocity commands or acceleration commands depending on the type of the automatic flight control modes available on a specific vehicle. Thus, the slung load controller is synthesized as a trajectory command generator.

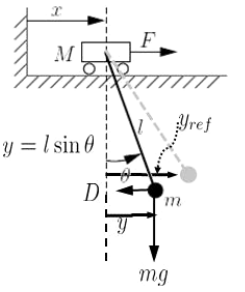

2.2. *System dynamics*

For simplicity, a helicopter flying with a slung load can be represented as a cart/pendulum model as shown in

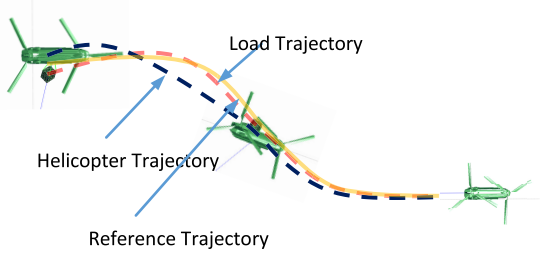

Fig. 1. The concept of the slung-load controller.

Un. Sys. 2016.04:213-226. Downloaded from www.worldscientific.com
by NATIONAL UNIVERSITY OF SINGAPORE on 12/14/16. For personal use only.

Fig. 2. Sketch of GTMax with slung load and its simplified representative model of cart/pendulum.

Fig. 2. In the simplified model, the cart (helicopter center of mass) is assumed to move in the horizontal plane with the load attached to the cart by a massless rigid link. Figure 2 depicts the simplified model for longitudinal motion along the inertial x-axis. A similar simplified model for the lateral motion of the helicopter is used for the control law development.

It is apparent that there are many differences between the real and the simplified model. But the cart/pendulum model has been considered to be sufficient for controller synthesis since it can represent well the macroscopic oscillation of a slung load and the coupled motion between helicopter and load.

The nonlinear equation for the pendulum dynamics can be obtained as

$$\ddot{\theta} = -\frac{g\sin\theta}{l} - \frac{\cos\theta}{l}\ddot{x} - \frac{\cos\theta}{l}\frac{D}{m}, \tag{1}$$

where x is the horizontal position of cart, θ is the angular position of the load, m is the mass of the load, and D is drag force on the load. The drag force D is assumed to be horizontal in the simplified model.

2.3. *The slung-load controller*

The objective of the slung load controller is to position the load over a moving target such as a moving truck or a moving ship deck, while damping the load oscillations. In order to accomplish the stated objective, the slung load controller is conceptualized as an outer loop controller to the vehicle flight control system. The output of the slung load controller is commanded vehicle acceleration which is used to generate trajectory command input to the vehicle flight control system. The acceleration command is constructed using a combination of load oscillation control part and target position tracking part.

2.3.1. *Load oscillation controller*

The load oscillation control part is used to regulate the load relative position from the center of the vehicle (y shown in Fig. 2) to be close to a reference value. Denoting a_{oc} as the load oscillation controller part of the commanded acceleration of the vehicle along the inertial x-axis, an equation for a_{oc} is obtained from feedback linearization of load dynamics as detailed in the following. Starting with the equation for the relative position of the load position from the vehicle center along the inertial x-axis, i.e.,

$$y = l\sin\theta. \tag{2}$$

Equation (2) is differentiated twice to get

$$\ddot{y} = \ddot{\theta}l\cos\theta - l\dot{\theta}^2\sin\theta. \tag{3}$$

Substituting for $\ddot{\theta}$ from Eq. (1) into Eq. (3), one gets

$$\begin{aligned}\ddot{y} &= -\ddot{x}\cos^2\theta - \frac{D}{m}\cos^2\theta - g\cos\theta\sin\theta - l\dot{\theta}^2\sin\theta \\ &= \nu.\end{aligned} \tag{4}$$

In Eq. (4), $\ddot{y}$ is equated to a pseudo control ν. Replacing $\ddot{x}$ by a_{oc} in Eq. (4), one obtains the following control law for a_{oc} from the inverse of Eq. (4).

$$a_{oc} = -\left(\nu + l\dot{\theta}^2\sin\theta + g\cos\theta\sin\theta + \frac{D}{m}\cos^2\theta\right)\frac{1}{\cos^2\theta}. \tag{5}$$

Next, the pseudo control, ν, is obtained as the output of a static compensator given by the following equation

$$\nu = -k_{\dot{y}}(\dot{y} - \dot{y}_{ref}) - k_y(y - y_{ref}). \tag{6}$$

Thus, the nonlinear oscillation control law is constructed by combining Eqs. (5) and (6). In the actual implementation of the control law given by Eq. (5), the drag force on the load D is replaced by an estimate using $D_{estimate} = \frac{1}{2}\rho V^2 f$, where ρ is air density, V is speed of load along the inertial x-axis ($V = |\dot{x} + \dot{y}|$) and f is an estimate of the equivalent

Un. Sys. 2016.04:213-226. Downloaded from www.worldscientific.com
by NATIONAL UNIVERSITY OF SINGAPORE on 12/14/16. For personal use only.

flat plate drag area of the load. In Eq. (6), the value of $\dot{y}_{\text{ref}}$ is taken to be zero and y_{ref} is obtained using steady state angular position of the load θ_{ss}

$$\begin{aligned} \theta_{ss} &= -\tan^{-1}\frac{\hat{D}}{mg}, \\ y_{\text{ref}} &= l\cos\theta_{ss}, \end{aligned} \tag{7}$$

where $\hat{D}$ is an estimate of the drag force on the load in the absence of load oscillations, i.e., speed of load equals that of the vehicle. The equations for the load oscillation controller presented above are formulated for the longitudinal and lateral motions in the inertial frame separately.

2.3.2. *Target position tracker*

As previously stated in the introduction, the output of the nonlinear oscillation controller, Eqs. (5) and (6), is combined with the output of a target position tracker. Denoting a_{pd} as the target tracker part of the commanded acceleration of the vehicle along the inertial x-axis, the target position tracker is constructed in terms of a linear PD control law as

$$a_{pd} = -K_v(\dot{\hat{x}}_L - \dot{x}_T) - K_p(\hat{x}_L - x_T), \tag{8}$$

where $\dot{x}_T, x_T$ are the target velocity and position along the inertial x-axis, $\dot{\hat{x}}_L, \hat{x}_L$ are the estimated steady state velocity and position of the slung-load along the inertial x-axis, and K_v, K_p are velocity and position gains. The estimated steady state load velocity and position, $\dot{\hat{x}}_L, \hat{x}_L$ along the inertial x-axis are obtained using

$$\dot{\hat{x}}_L = \dot{x}, \quad \hat{x}_L = x + l\tan^{-1}\frac{\hat{D}}{mg} \tag{9}$$

where $\hat{D}$ is an estimate of the drag force on the load in the absence of load oscillations, i.e., speed of load equals that of the vehicle. Once again, the equations for the target tracker presented above are formulated in the longitudinal and lateral motions in the inertial frame separately.

2.3.3. *Composite controller*

The composite control law is obtained by combining the synthesized control laws of the target tracker and the load oscillation controller from the above as

$$a_c = k_1 a_{pd} + k_2 a_{\text{oc}}, \tag{10}$$

where a_c is the total commanded acceleration of the vehicle, a_{oc} is the acceleration command from the load oscillation controller (Eq. (5)), a_{pd} is the acceleration command from the target tracker (Eq. (8)), and k_1 and k_2 are the merging factors whose values are selected based on the flight phase as explained below.

The target tracking is divided into three phases, viz., far tracking, near tracking and fine tracking. The far tracking phase is considered to be active when the vehicle is farther than roughly 100 ft from the target. The near tracking phase is considered to be active when the vehicle position is in the range of roughly 100∼5 ft from the target and the fine tracking phase is considered to be active when the vehicle position is within roughly 5 ft of the target position. During the far and near tracking phases, greater emphasis is placed on load oscillation damping, whereas during the fine tracking phase, greater emphasis is placed on target tracking. During the far tracking and near tracking phases, the commanded position and velocity, if needed, are obtained by integrating the commanded acceleration.

$$\begin{aligned} \dot{x}_c(t+\Delta t) &= \dot{x}(t) + \int_t^{t+\Delta t} a_c(t)dt, \\ x_c(t+\Delta t) &= x(t) + \int_t^{t+\Delta t} \dot{x}_c(t)dt. \end{aligned} \tag{11}$$

During the fine tracking phase, the current target velocity and position are used to obtain the position and velocity commands, respectively.

$$\begin{aligned} \dot{x}_c(t+\Delta t) &= \dot{x}_T(t) + \int_t^{t+\Delta t} a_c(t)dt, \\ x_c(t+\Delta t) &= x_T(t) + \int_t^{t+\Delta t} \dot{x}_c(t)dt. \end{aligned} \tag{12}$$

Figure 3 shows a schematic structure of the proposed active slung load controller. The Mode decision block is made up of three distinct modes, viz., normal mode, position hold mode, and emergency mode. In the case of emergency mode of operation, the target position tracker is turned off and only the nonlinear oscillation controller is used to quickly damp out any dangerous load oscillations. In the case of position hold mode, the filtered target position values provided to the slung load controller are frozen to those values just prior to the selection of this mode and the emphasis on target tracking is decreased by reducing the value of k_1 by a preselected value. In the normal mode, the individual commands from the target tracker and the load oscillation damper are merged using Eq. (10).

2.4. *Adaptive neural network for slung load control*

The control laws presented in Eqs. (5)–(10) use physical parameters such as mass of load, mass of helicopter, cable length, estimated drag acting on the load, etc., which can be different for different slung load missions. The controller

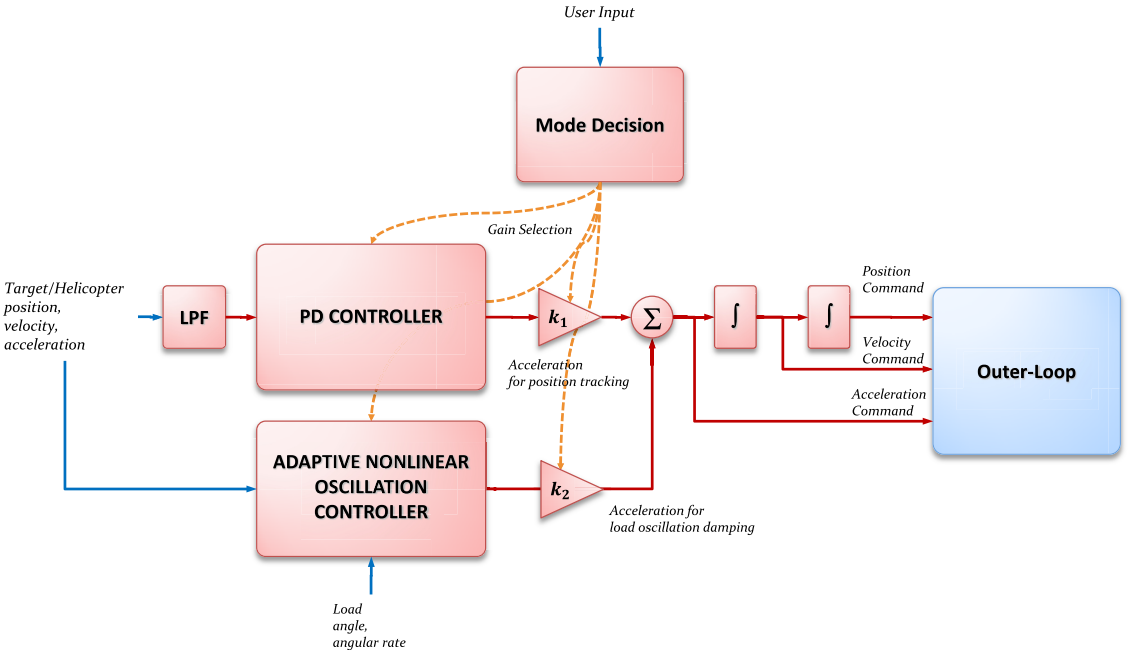

Fig. 3. Schematic structure of the proposed slung-load controller.

gains of the target tracker and the load oscillation damper are selected based on a nominal set of slung load system parameters. In order to compensate for the effects of uncertainties such as parameter changes, model approximations, external gust effects, etc., the load oscillation controller is augmented with an adaptive neural net as described below.

Considering the dynamics of the load position relative to the vehicle given in Eq. (4) as an approximation, the true dynamics of the load position relative to the vehicle can be expressed as

$$\ddot{y} = \nu + \Delta, \tag{13}$$

where Δ represents the model error in using Eq. (4) for load dynamics. Instead of using the pseudo control given by Eq. (6), one can define a new pseudo control that includes an adaptive term as

$$\nu \triangleq \ddot{y}_{\text{ref}} + \nu_{sc} - \nu_{ad} \tag{14}$$

where the pseudo control in Eq. (6) is redefined as a static pseudo control

$$\nu_{sc} = K_{\dot{y}}(\dot{y} - \dot{y}_{\text{ref}}) - K_y(y - y_{\text{ref}}). \tag{15}$$

Now, substituting Eqs. (14) and (15) into Eq. (13) results in the following error dynamics equation:

$$\dot{e} = \begin{bmatrix} 0 & 1 \\ -K_y & -K_{\dot{y}} \end{bmatrix} e + \begin{bmatrix} 0 \\ 1 \end{bmatrix} (\Delta - \nu_{ad}) = Ae + b(\Delta - \nu_{ad}) \tag{16}$$

where the error vector is $\mathbf{e} = [(y - y_{\text{ref}})(\dot{y} - \dot{y}_{\text{ref}})]^T$. Since the system matrix A of Eq. (16) is Hurwitz, the error dynamics is asymptotically stable. Further, as the adaptive term approaches the model error, that is $\nu_{ad} \to \Delta$, then the output error $e \to 0$.

2.5. *Adaptive neural network*

A single-hidden-layer (SHL) neural network (NN) is used to approximate the uncertainty term Δ in Eq. (13). Reference [9] establishes a universal approximation for an unknown continuous function of states and control in a bounded, observable process using a memory unit of sampled input/output pairs. Figure 4 shows the generic structure of a SHL NN.

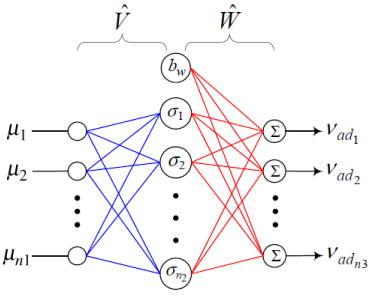

Fig. 4. Generic structure of a SHL NN.

Un. Sys. 2016.04:213-226. Downloaded from www.worldscientific.com
by NATIONAL UNIVERSITY OF SINGAPORE on 12/14/16. For personal use only.

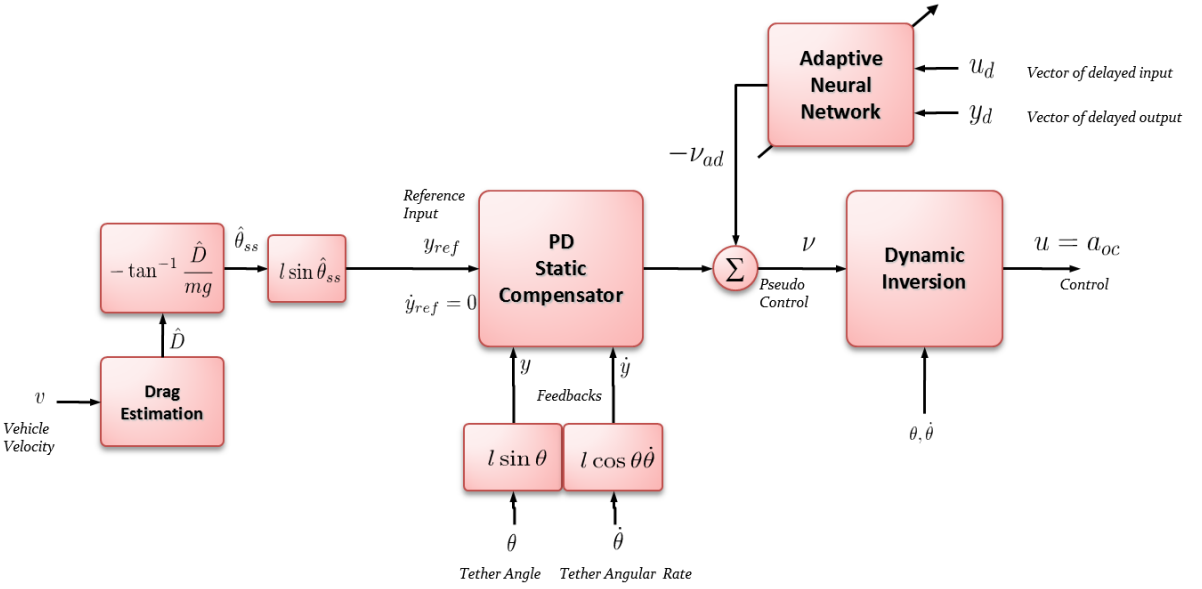

Fig. 5. Schematic structure of the adaptive nonlinear oscillation controller.

The SHL NN weights are updated on-line using the adaptive law given by [9]

$$\begin{aligned} \dot{\hat{W}} &= -\Gamma_W[2(\sigma - \sigma')\mathbf{e}\ \mathbf{p}\ \mathbf{b} + k_w\hat{W}], \\ \dot{\hat{V}} &= -\Gamma_V[2\,\bar{\mu}\mathbf{P}\mathbf{b}\hat{W}^T\sigma' + k_v\hat{V}], \end{aligned} \tag{17}$$

where $\Gamma_W > 0$ and $\Gamma_V > 0$ are adaptation gains for the output layer weights $\hat{W}$ and the hidden layer weights $\hat{V}$, respectively. In addition, σ denotes basis function, b is bias term, σ' denotes the Jacobian matrix, $\mathbf{P}$ is the solution of the Lyapunov equation with given $\mathbf{Q} > 0$,

$$\mathbf{A}^T\mathbf{P} + \mathbf{P}\mathbf{A} = \mathbf{Q}. \tag{18}$$

$k_W > 0$ and $k_V > 0$ are the sigma modification gains, and μ represents the NN input vector defined as

$$\bar{\mu} = \begin{bmatrix} 1 & u_d^T & y_d^T \end{bmatrix}^T, \tag{19}$$

where u_d^T and y_d^T are the delayed input and output vector, respectively,

$$\begin{aligned} u_d^T &= [u(t) \quad u(t - \Delta t)], \\ y_d^T &= [y(t) \quad \dot{y}(t) \quad y(t - \Delta t) \quad \dot{y}(t - \Delta t)], \end{aligned}$$

and Δt is time delay.

Figure 5 shows the overall structure of the nonlinear slung load oscillation damper with an adaptive NN. The output y and the reference output y_{ref} are calculated inside the controller from the measured tether angle, estimated drag, and estimated bias error.

3. Test and Evaluation

3.1. *Onboard software implementation on a UAV*

The proposed slung load controller algorithms are integrated into the onboard computer of the GTMax unmanned helicopter. The GTMax rotary-wing test-bed (see Fig. 6) is a modified Yamaha RMax helicopter that uses a unique integrated simulation and flight test architecture. Detailed descriptions of the GTMax hardware configuration are provided in [10, 11].

A block diagram representation of the integration of the proposed slung load controller with the GTMax trajectory following controller [12] architecture is shown in Fig. 7. The slung load controller provides trajectory commands

Fig. 6. The Georgia Tech UAV test-bed: GTMax.

Un. Sys. 2016.04:213-226. Downloaded from www.worldscientific.com
by NATIONAL UNIVERSITY OF SINGAPORE on 12/14/16. For personal use only.

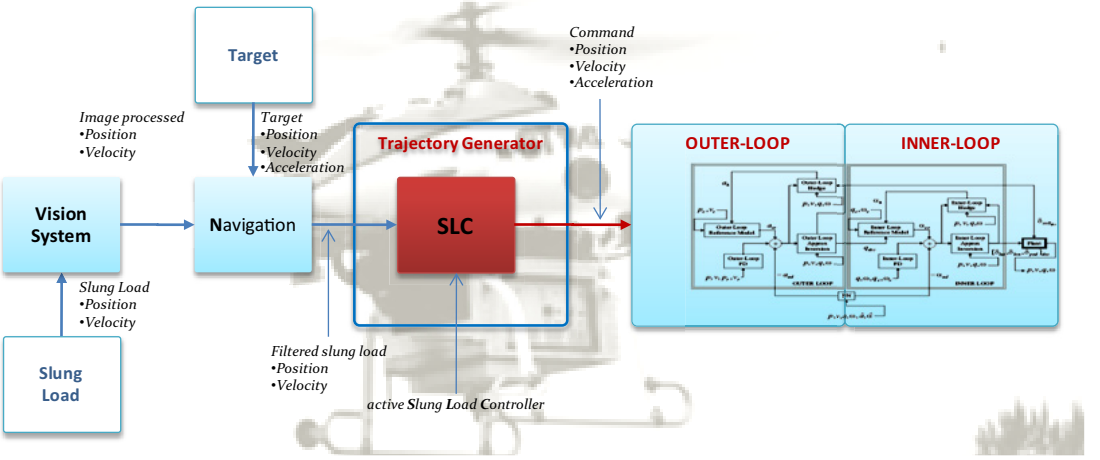

Fig. 7. Integration of the slung-load controller with the GTMax onboard flight controller.

Un. Sys. 2016.04:213-226. Downloaded from www.worldscientific.com
by NATIONAL UNIVERSITY OF SINGAPORE on 12/14/16. For personal use only.

to the outer loop of the GTMax flight controller. The GTMax flight controller is an adaptive NN trajectory following controller with 18 NN inputs, 5 hidden layer neurons, and 7 outputs for each of the 7 degrees of freedom. The 7 degrees of freedom include the usual 6 rigid-body degrees of freedom plus a degree of freedom for rotor RPM. The navigation system is a 17 state Extended Kalman Filter that fuses information from 5 related sensors (GPS, IMU, sonar, radar, and magnetometer) to provide estimates of vehicle position, velocity, attitude, and terrain height. The flight controller determines actuator commands based on the outputs of the navigation system and guidance commands. The GTMax helicopter model, the helicopter interface model, and sensor models have been developed as a simulation tool called the Georgia Tech UAV Simulation Tool (GUST) [11]. This simulation tool is written primarily in C/C++ and has been developed to allow the test architecture to run on a high-end personal computer.

The position of the slung-load is detected and filtered through a vision system called SLIP (slung-load image processor), which is composed of a down-looking camera, image processing algorithm that detects the attached circular shape on upper surface of the slung-load, and a Kalman filter based filter to estimate the oscillatory position and velocity of the slung-load from the measurements by the image processing algorithm.

3.2. *Simulations*

The performance of the proposed active slung load controller is first evaluated in simulation using a nonlinear model of the GTMax unmanned helicopter within the GUST. The values of the controller gains and related system parameters selected are given in Table 1.

Table 1. Gain/Parameter selection for the active slung load controller in fine tracking mode.

Gain/ Parameters	Description	Value
K_p	Position gain	0.15
K_v	Velocity gain	0.20
K_y	Load position gain	4.00
$K_{\dot{y}}$	Load velocity gain	1.00
M	Vehicle mass (slugs)	4.88
m	Load mass (slugs)	0.6
f	Load equivalent flat plate drag area (ft^2)	1.0
l_c	Tether length (ft)	30
Γ_W	Output layer adaptation gain	0.08
Γ_V	Hidden layer adaptation gain	0.08
k_V	σ-modification gain	1.0
k_W	σ-modification gain	1.0
Q	p.d. matrix	$I_{2\times 2}$
P	[0.75 −0.5 −0.5 2.5]	
Merging factors	Far Tracking : $k_1 = 0.16$, $k_2 = 1$ Near tracking : $k_1 = 0.23$, $k_2 = 1$ Fine tracking : $k_1 = 0.3$, $k_2 = 1$	

Simulation evaluations are carried out with and without the adaptive neural net block in the slung load controller. Also, different cases of uncertainty in terms of error in load parameter estimates, external gusts, and random target motion are considered in the simulation. A summary of various cases considered are given in Table 2.

The ground vehicle position and velocity are simulated by integrating its assumed initial values of heading direction and speed for the nominal case. For the random target (ground vehicle) motion case considered in Table 7, the ground vehicle position and velocity are simulated through

Table 2. Summary of simulation cases.

Symbol	Description	Nominal	Case 1	Case 2	Case 3	Case 4	Case 5
NN		*off*	*off*	*on*	*off*	*on*	←
Measurement errors							
	Load position error (deg)	0	−2°	←	←	←	←
Slung load configuration errors							
M	Vehicle mass (slugs)	5.16 (full)	←	←	←	←	←
m	Load mass (slugs)	0.6	0.48	←	←	←	←
C_{D_0}	Load drag coefficient	1.0	1.20	←	←	←	←
l_c	Tether length (ft)	30	36.0	←	←	←	←
Environment							
$\vec{v}_g$	Wind gust (ft/s)	off	off	off	15 ft/s	←	←
$\vec{v}_w$	Steady wind (ft/s)	off	off	off	NW 5 ft/s	←	←
$\vec{p}_T, \vec{v}_T, \vec{a}_T$	Target movement	Const. 15 ft/s to north	←	←	←	←	Gauss–Markov random acc.

Note: ← represents "value equals that show on the left".

integration of random accelerations generated by the Markov process. The position and velocity of ground vehicle are assumed to be transferred to the UAV via a data-link. The nominal case assumes an accurate knowledge of the slung load parameters. For the nominal case, the target is assumed to be moving at a constant speed of 15 ft/s along a straight line. Figures 8(a)–8(c) show example scenes from the simulation for the nominal case during far tracking, near tracking, and fine tracking phases, respectively. In Fig. 8, the ground vehicle is colored in red and UAV position command determined by the slung-load controller is represented as the yellow circle.

Figures 9–12 summarize the simulation results for the nominal case and for the cases 1 through 5. Subplots in each of these figures show errors in position and velocity of the load relative to the target position and velocity and a captured scene of the simulation during the fine tracking phase.

From these results, it is seen that the active slung load controller works well in dampening the load oscillation significantly even for the worst case (case 5), which includes parametric uncertainty, external turbulence, and random target motion. With the adaptive neural net turned on, the position error stays within 6 ft and the velocity error stays within 3 ft/s as seen from case 5 plots in Fig. 12.

A comparison between plots for cases 1 and 2 in Fig. 10 or cases 3 and 4 in Fig. 11 reveals the effectiveness of the adaptive neural net in reducing the resulting bias errors due to parametric uncertainty and/or external gusts. However, since more emphasis is placed on target tracking during the fine tracking phase, the transient load motions during this phase, especially in the presence of external gusts and random ground vehicle motion, may not be acceptable, even though the average position and velocity errors are reduced.

3.3. *Flight test*

Preliminary flight tests were carried out to test the effectiveness of the proposed slung load controller without

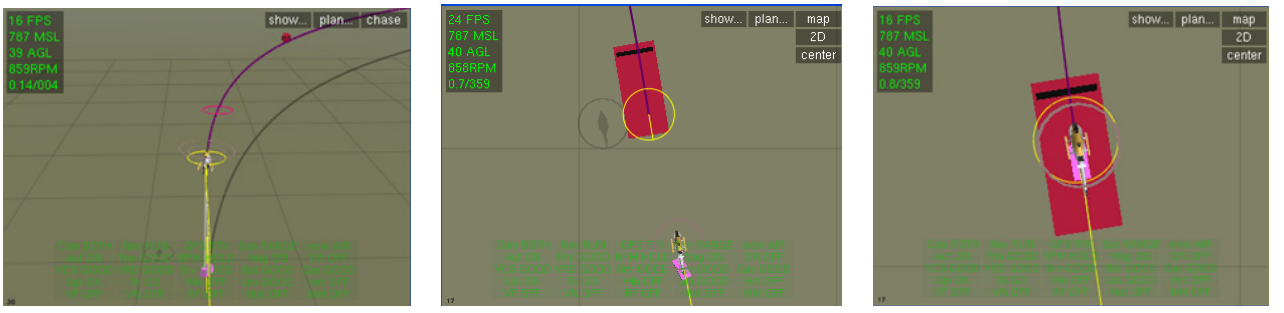

(a) (b) (c)

Fig. 8. Simulation scenes during target tracking for the nominal case. (a) Far tracking phase, (b) Near tracking phase and (c) Fine tracking phase.

Un. Sys. 2016.04:213-226. Downloaded from www.worldscientific.com
by NATIONAL UNIVERSITY OF SINGAPORE on 12/14/16. For personal use only.

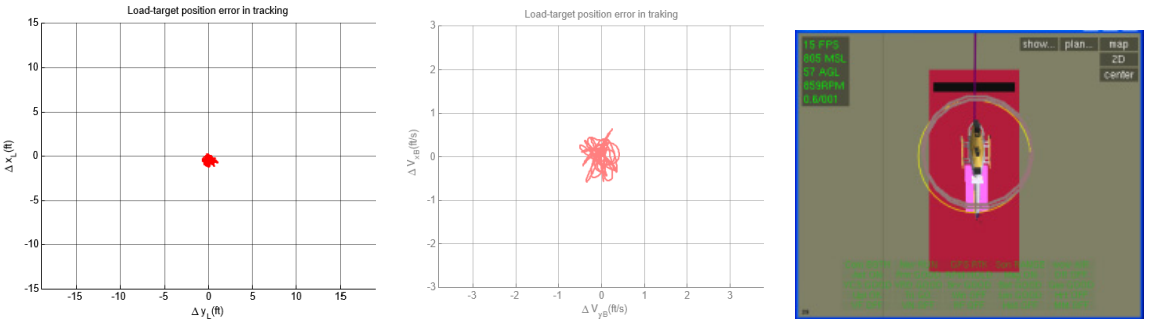

(a) (b) (c)

Fig. 9. Simulation results for the nominal case. (a) Position error between target and slung-load, (b) Velocity error between target and slung-load and (c) Captured scene.

Un. Sys. 2016.04:213-226. Downloaded from www.worldscientific.com
by NATIONAL UNIVERSITY OF SINGAPORE on 12/14/16. For personal use only.

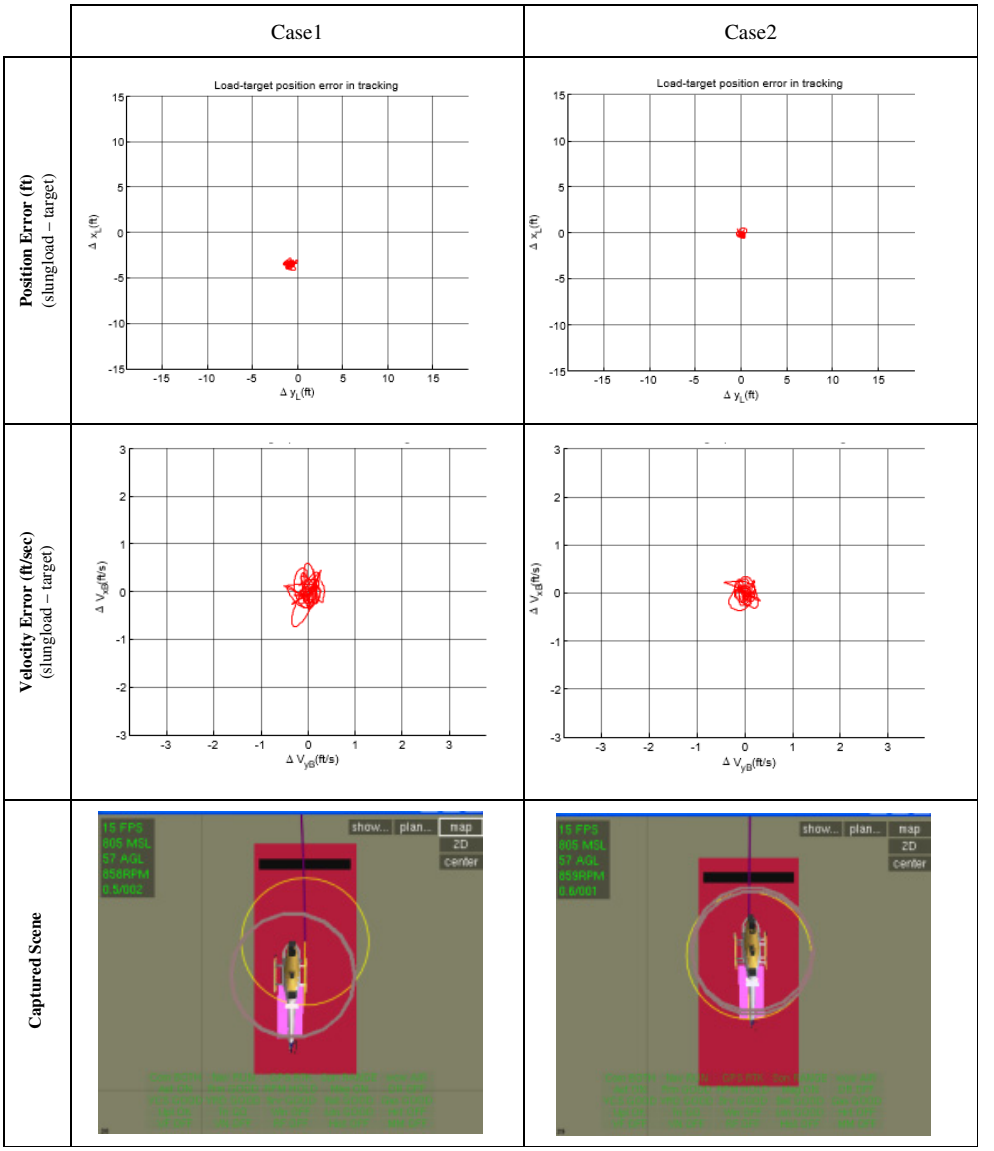

Fig. 10. Simulation results for cases 1 and 2.

Un. Sys. 2016.04:213-226. Downloaded from www.worldscientific.com
by NATIONAL UNIVERSITY OF SINGAPORE on 12/14/16. For personal use only.

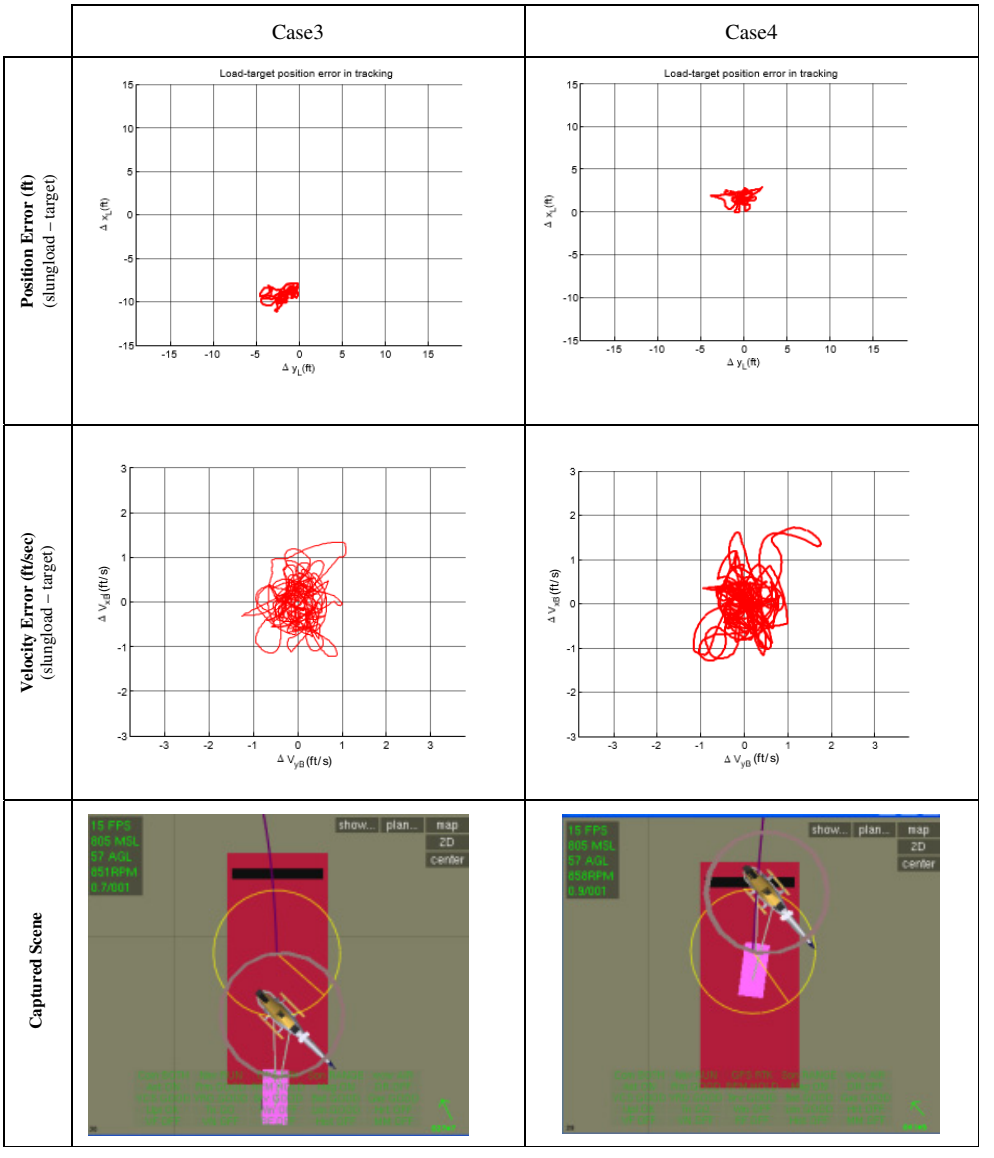

Fig. 11. Simulation results for cases 3 and 4.

the adaptive neural net in tracking a virtual ground vehicle during the fine tracking phase. For this purpose, a previously developed vision system with image processing and object recognition software was used for the measurement of slung load position and velocity. During the flight test, ground vehicle's motion was simulated in a separate computer and the simulated position and velocity were transmitted to GTMax via the data-link. A picture of the GTMax with a slung load used in the limited tests is shown in Fig. 13.

The flight test results for the case with the slung load oscillation controller turned off are shown in Figs. 14(a) (planar trajectory) and 14(b) (load-target position error). Similar results from flight tests for the case with the slung load oscillation controller turned on are shown in Figs. 15 (a) (planar trajectory) and 15(b) (load-target position error). For comparison, simulation results with the slung load oscillation controller turned on are shown in Figs. 16 (a) (planar trajectory) and 16(b) (load-target position error). In Figs. 14(a), 15(a) and 16(a), the virtual ground vehicle inertial position (labeled as tgt), the vehicle inertial *xy*-position (labeled as GTMax) and the load inertial *xy*-position (labeled as load) are compared with one another for each case. Figures 14(b), 15(b) and 16(b) compare error in tracking of the moving target by the load. A comparison of the flight test results with and without the slung load controller (Figs. 14(b) and 15(b)) shows that the slung load controller is effective in suppressing the load oscillations

Un. Sys. 2016.04:213-226. Downloaded from www.worldscientific.com
by NATIONAL UNIVERSITY OF SINGAPORE on 12/14/16. For personal use only.

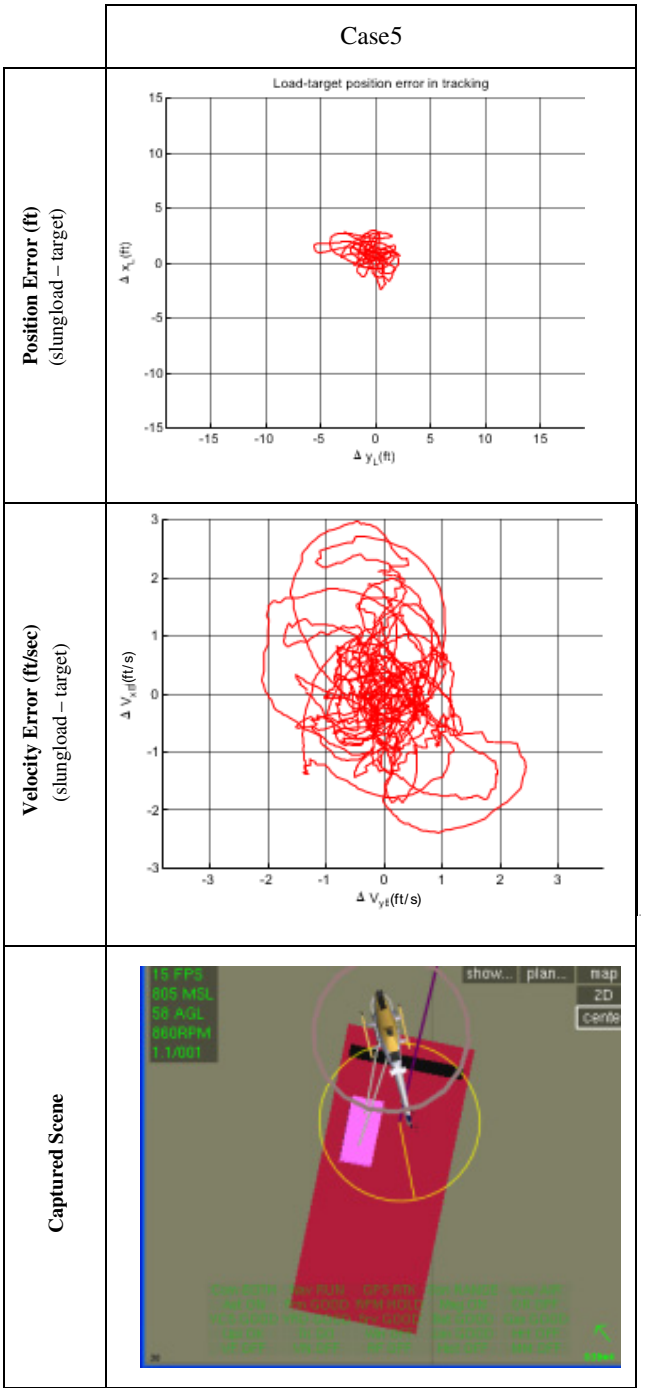

Fig. 12. Simulation results for case 5.

while doing a reasonable job in tracking the ground vehicle. Further, it is seen that the simulation and flight test results with the slung load controller (Figs. 15 and 16) exhibit similar performance in suppressing load oscillations. However, the magnitude of the tracking errors in flight tests is seen to be larger than those from the simulation results. It is to be noted that the simulation results shown here for the

Fig. 13. GTMax is flyinf with a slung-load during the flight test.

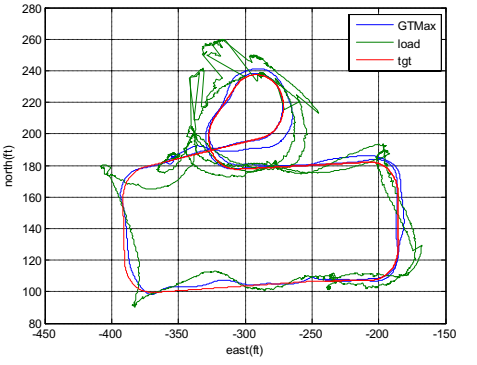

(a)

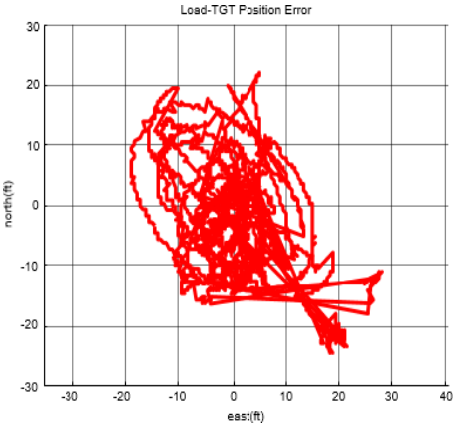

(b)

Fig. 14. Planar trajectory and load-target position error from flight test with slung load oscillation controller turned off. (a) Planar trajectory and (b) Load-target position error.

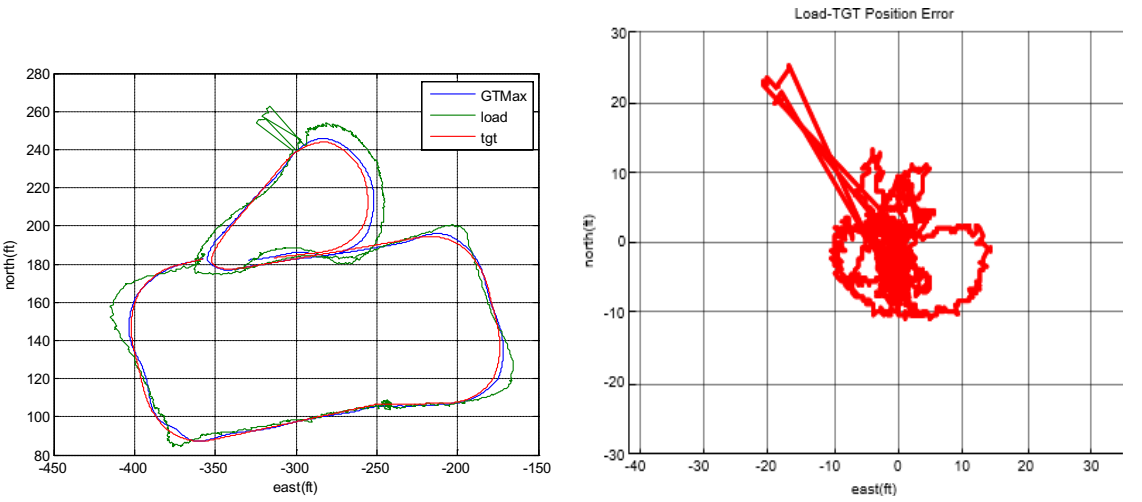

(a) (b)

Fig. 15. Planar trajectory and load-target position error from flight test with slung load oscillation controller turned on. (a) Planar trajectory and (b) Load-target position error.

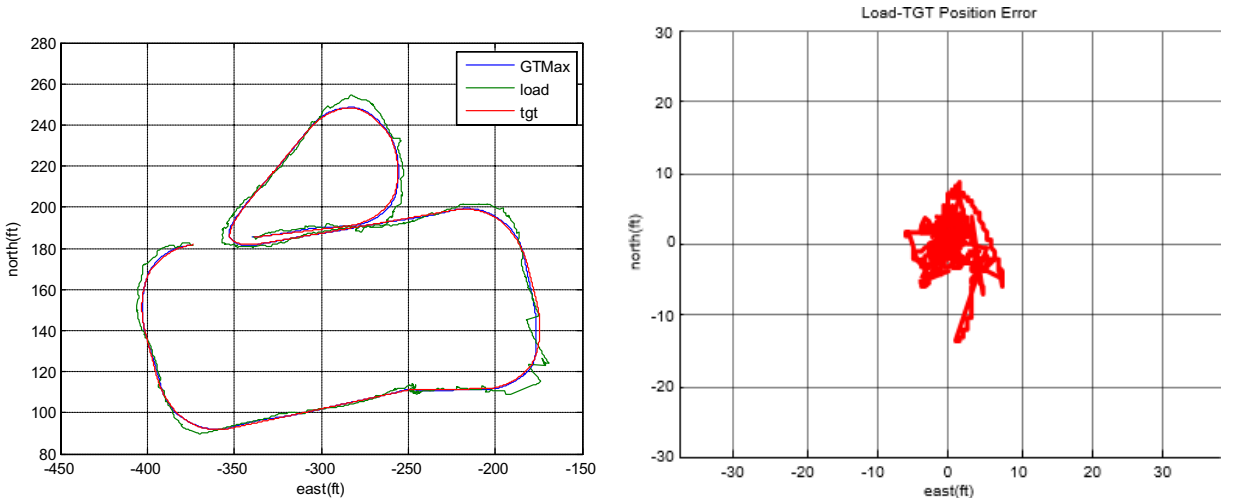

(a) (b)

Fig. 16. Planar trajectory and load-target position error from simulation for the nominal case with slung load oscillation controller turned on. (a) Planar trajectory from simulation for the nominal case and (b) Load-target position error from simulation for the nominal case.

nominal case do not include the effects of any uncertainties while the actual flight results are affected by uncertainties.

4. Concluding Remarks

This paper presents the synthesis, design, and testing of a slung load controller for the precision delivery of an externally carried load by an unmanned helicopter onto a moving ground vehicle or a moving ship deck. The proposed slung load controller is composed of three parts, viz., a target position tracker, a nonlinear load oscillation damper, and an adaptive neural net block. The target position tracker is made up of a linear PD controller which generates an acceleration command to track a moving target. The nonlinear slung load oscillation damper is based on feedback linearization of the nonlinear dynamics of the slung load system. The nonlinear oscillation damper is augmented with an adaptive neural net block to accommodate uncertainty associated with modeling errors, external gusts, and random ground vehicle motion. The performance of the

Un. Sys. 2016.04:213-226. Downloaded from www.worldscientific.com
by NATIONAL UNIVERSITY OF SINGAPORE on 12/14/16. For personal use only.

proposed controller is evaluated in simulations using a nonlinear model of the GTMax helicopter UAV test-bed within the GUST. Further, preliminary flight tests of the proposed slung load controller without the adaptive neural net block are carried out using the GTMax UAV helicopter test-bed with a representative slung load and a virtual ground vehicle. Both the simulation results and the flight test results demonstrate the performance of the proposed slung load controller in suppressing load oscillations while achieving reasonable performance in tracking of the ground vehicle by the load.

The evaluations carried out in this work include only moderate amounts of uncertainties associated with system parameters, external gusts, and random ground vehicle motion. While the performance of the proposed controller is shown to be reasonable in the presence of moderate amounts of uncertainty, it is expected that the tracking performance of the controller will degrade much more in the presence of severe external gusts and/or larger variations in ground vehicle motions than what has been modeled in this study. Fundamentally, such degradation is inevitable with a controller regulating load position error via vehicle motions. While a direct mechanism for load position controller, for example, controlled thrusters mounted on the load, etc., can result in better tracking performance, the presented scheme of controlling load position via vehicle motions is logistically simpler. Thus, a careful trade-off between performance and system complexity is needed in order to arrive at a satisfactory solution. This needs to be addressed in future studies.

Un. Sys. 2016.04:213-226. Downloaded from www.worldscientific.com
by NATIONAL UNIVERSITY OF SINGAPORE on 12/14/16. For personal use only.

Acknowledgments

This work was funded under a DARPA seedling project at the Georgia Institute of Technology with Mr. Daniel Newman as the Technical Monitor.

References

[1] R. H. Hoh, R. K. Heffley and D. G. Mitchell, Development of handling quality criteria for rotorcraft with externally slung loads, NASA-CR-2006-213488, NASA Ames Research Center (2006).

[2] L. Cicolani and G. Kanning, Equation of motion of slung-load systems with results for dual lift, NASA-TM-102246 (1990).

[3] L. Cicolani and G. Kanning, Equation of motion of slung-load systems, including multilift systems, NASA-TP-3280 (1992).

[4] R. Raz, A. Rosen and T. Ronen, Active aerodynamic stabilization of a helicopter/sling-load system, *AIAA J. Aircraft* **26**(9) (1989) 822–828.

[5] M. Bisgaard, J. D. Bendtsen and A. Cour-Harbo, Modeling of generic slung load system, *AIAA Modeling and Simulation Technologies Conf. Exhibit*, AIAA-2006-6816 (Washington DC, 2006).

[6] M. Bisgaard, A. Cour-Harbo and J. D. Bendtsen, Input shaping for helicopter slung load swing reduction, *AIAA Guidance, Navigation and Control Conf. and Exhibit*, AIAA-2008-6964 (Washington DC, 2008).

[7] M. Bisgaard, Modeling, estimation, and control of helicopter slung load system, Ph.D. Thesis, Aalborg University, Denmark (2008).

[8] J. Yu, F. L. Lewis and T. Huang, Nonlinear feedback control of a gantry crane, in *Proc. American Control Conf.*, Seattle, June 1995, pp. 4310–4315.

[9] N. Hovakimyan, A. J. Calise and N. Kim, Adaptive output feedback control of a class of multi-input multi-output systems using neural networks, *Int. J. Control* **77**(15) (2004) 1318–1329.

[10] E. N. Johnson and D. P. Schrage, The Georgia Tech Unmanned Aerial Research Vehicle: GTMax, *AIAA Guidance, Navigation and Control Conf. and Exhibit*, AIAA-2003-5741 (Washington DC, 2003).

[11] E. N. Johnson, D. P. Schrage, J. V. R. Prasad and G. J. Vachtsevanos, UAV Flight Test Programs at Georgia Tech, in *Proc. AIAA* "*Unmanned Unlimited*" *Technical Conf., Workshop, and Exhibit* (2004).

[12] E. N. Johnson and S. K. Kannan, Adaptive trajectory control for autonomous helicopters, *AIAA J. Guidance Control Dyn.* **28**(3) (2005) 524–538.

Keeryun Kang is a senior researcher at Agency for Defense Development (ADD), Daejeon, South Korea. He is currently working in the area of system integration of an unmanned system. Keeryun Kang received the B.S. and M.S. degrees in the School of Aerospace Engineering at Inha University, Incheon, South Korea, in 1995 and 1997, respectively, and received Ph.D. degree at Georgia Institute of Technology, Atlanta, GA, USA, in 2012. He has numerous research experiences in 6DOF simulation of aerial system, guidance, and control algorithm design, the system integration, hardware-in-the-simulation of control algorithms, and the conceptual design and simulation of unmanned system. His areas of interest are adaptive control, trajectory optimization, optimal control, aerial unmanned vehicle dynamics, and flight simulation.

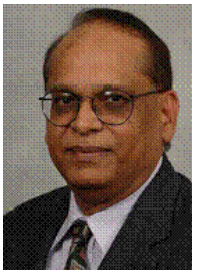

J.V.R. Prasad is a Professor in the School of Aerospace Engineering at the Georgia Institute of Technology working in the area of Flight Mechanics and Control. He received his B.Tech degree from the Indian Institute of Technology, Madras, India and his M.S and Ph.D. degrees from the Georgia Institute of Technology, Atlanta, USA. He is currently a Co-Principal Investigator and an Associate Director for the US Army sponsored Vertical Lift Rotorcraft Center of Excellence (VLRCOE) program and a Co-Principal Investigator for the Pratt & Whitney Center of Excellence program at Georgia Tech. He has extensive research and design experience in rotorcraft system modeling and control, propulsion system modeling and control, and autonomous air vehicle modeling and control. He is the recipient of the 2009 ASME Melville Medal. He served as the Editor-In-Chief of the Journal of the American Helicopter Society. He currently serves as a member of the Editorial Board for the International Journal on Mathematical Modeling and Simulation and the Advisory Board for the International Journal of Unmanned Systems. He is a Fellow of the AIAA, a Technical Fellow of the AHS and a Member of the ASME.

Eric N. Johnson is the Lockheed Martin Associate Professor of Avionics Integration in the School of Aerospace Engineering at Georgia Institute of Technology, and Director of the UAV Research Facility. He is an Aerospace Engineer and Instrument-Rated Pilot, experienced in: guidance, navigation, control systems, aerodynamics, stability & control, flight simulation (including dynamic modeling and scene generation), aerospace software, flight test, and human factors. His research interests include: fault tolerant estimation and control theory; and digital avionics system design and integration. He performs research sponsored by a variety of sources, including: The National Science Foundation, AFOSR, DARPA, NASA, AFRL/VACA, NIST, Sikorsky, and Lockheed Martin. Major research programs have included the Active-Vision Control Systems MURI and the Software Enabled Control program, as well as the development of several research Unmanned Aerial Vehicle (UAV) Systems. A majority of this research is conducted in the Unmanned Aerial Vehicle Research Facility at Georgia Tech. Highlights of their work has been neural network adaptive flight control of a large number of different aircraft, vision-based guidance, navigation, control (including GPS-denied operations), autonomous aggressive maneuvering, the first air-launch of a hovering aircraft, and automatic flight of an airplane all the way to zero airspeed and back to forward flight.

Un. Sys. 2016.04:213-226. Downloaded from www.worldscientific.com
by NATIONAL UNIVERSITY OF SINGAPORE on 12/14/16. For personal use only.